Journal of Biomolecular NMR, 6 (1995) 427–432
ESCOM

J-Bio NMR 322

Triple resonance HNCCCH experiments for correlating exchangeable and nonexchangeable cytidine and uridine base protons in RNA

Jean-Pierre Simorre[a], Grant R. Zimmermann[a], Arthur Pardi[a,*], Bennett T. Farmer II[b] and Luciano Mueller[b,*]

[a]*Department of Chemistry and Biochemistry, University of Colorado at Boulder, Boulder, CO 80309-0215, U.S.A.*
[b]*Bristol-Myers Squibb Pharmaceutical Research Institute, P.O. Box 4000, Princeton, NJ 08543-4000, U.S.A.*

Received 19 September 1995
Accepted 25 October 1995

Keywords: RNA; Heteronuclear; Assignment; Isotopically labeled

Summary

A set of triple resonance experiments is presented, providing through-bond H_2N/HN to H6 connectivities in uridines and cytidines in ^{13}C-/^{15}N-labeled RNAs. These connectivities provide an important link between the sequential assignment pathways for the exchangeable and nonexchangeable proton resonances in nucleic acids. Both 2D and pseudo-3D HNCCCH experiments were applied to a 30-nucleotide lead-dependent ribozyme, known as the leadzyme. The HN to H6 connectivities for three uridines in the leadzyme were identified from one 2D H(NCCC)H experiment, and the H_2N to H6 connectivities were identified for seven of the eight cytidines from the combination of a 2D H(NCCC)H and a pseudo-3D H(NCC)CH experiment.

The ability to synthesize uniformly ^{13}C-/^{15}N-labeled RNAs (Batey et al., 1992; Nikonowicz et al., 1992) and DNAs (Zimmer and Crothers, 1995) has prompted the development of a variety of multinuclear experiments for resonance assignment of isotopically labeled nucleic acids (for reviews see Dieckmann and Feigon, 1994; Pardi, 1995). For example, sugar proton and carbon resonances can be efficiently assigned by application of HCCH-COSY, -RELAY and -TOCSY experiments (Pardi and Nikonowicz, 1992; Nikonowicz and Pardi, 1993); intra-residue base to sugar connectivities can be made by application of $H_sC_sN_bC_bH_b$, $H_sC_sN_b$, $H_bN_bC_s$, $H_bN_bC_b$ and $H_sC_sN_bH_b$ experiments (Farmer et al., 1993,1994; Sklenář et al., 1993a,b; Tate et al., 1994); HCCH-TOCSY experiments can be used to correlate the H2 and H8 resonances in adenine bases (Legault et al., 1994; Marino et al., 1994a); and sequential resonance assignments can be made by HCP-type and ^{13}C-^{31}P and ^{1}H-^{31}P heteroTOCSY-type experiments (Kellogg et al., 1992; Heus et al., 1994; Marino et al., 1994b,1995; Wijmenga et al., 1995). Here we present novel 2D and pseudo-3D triple resonance HNCCCH experiments that provide through-bond NH/NH_2 to H6 connectivities for uridine and cytidine base protons in ^{13}C-/^{15}N-labeled RNAs. These connectivities constitute an important link between the sequential assignment pathways for the exchangeable and nonexchangeable proton resonances in nucleic acids, and complement recently developed methods for through-bond assignment of adenine base protons in ^{13}C-labeled RNA (Legault et al., 1994; Marino et al., 1994a). The HNCCCH experiments are applied to a 30-nucleotide lead-dependent ribozyme, known as the leadzyme, that has the structure shown in Fig. 1A (Pan and Uhlenbeck, 1992).

Figures 2A and 2B give the 2D H(NCCC)H pulse sequences for identifying H_2N/HN to H6 connectivities in pyrimidines. Since the uridine HN to H6 magnetization transfer involves the same number and types of steps as the cytidine H_2N to H6 transfer (see Fig. 1B), essentially the same pulse sequence can be applied to either uridines or cytidines. However, as discussed below, optimal results are obtained if separate experiments are acquired for uridines and cytidines, with slightly different pulse sequences. In the uridine-optimized 2D H(NCCC)H pulse sequence given in Fig. 2A, protons are frequency labeled

*To whom correspondence should be addressed.

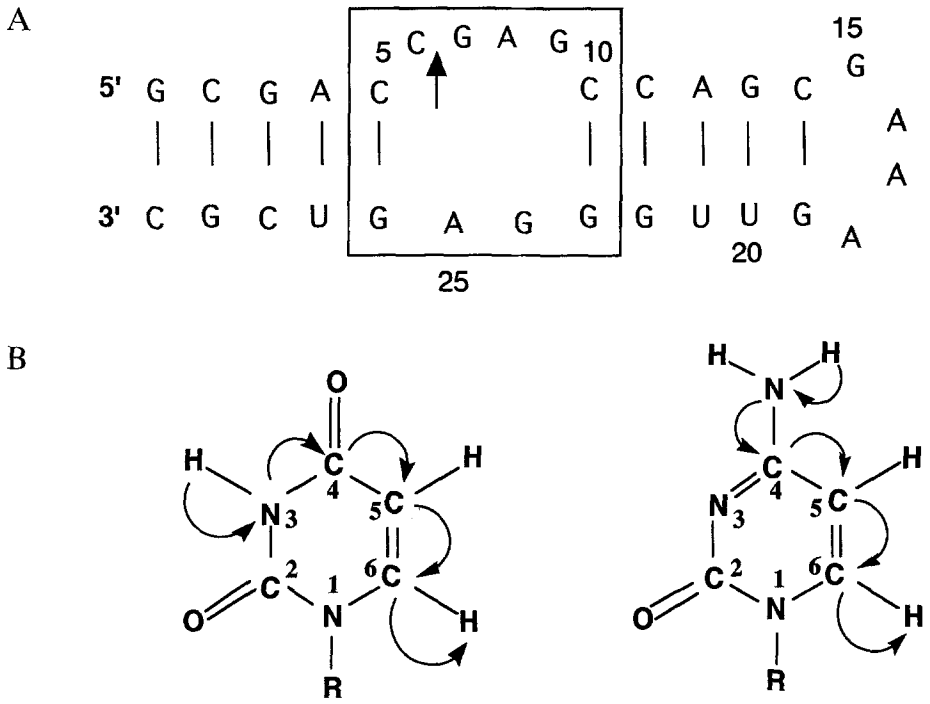

Fig. 1. (A) Sequence and secondary structure of the leadzyme (Pan and Uhlenbeck, 1992). The box indicates the nucleotides required for site-specific cleavage and the arrow indicates the cleavage site. (B) The uridine (left) and cytidine (right) magnetization transfer pathways employed in the HNCCCH experiments.

during the t_1 period and magnetization is transferred to nitrogen by a refocused INEPT sequence (Morris and Freeman, 1979). Next, magnetization is transferred to C4 by a ^{13}C-^{15}N-heteroTOCSY sequence (Bertrand et al., 1978; Mueller and Ernst, 1979). The high selectivity inherent in the heteroTOCSY sequence makes this the method of choice for the nitrogen to carbon magnetization transfer, especially in uridines where it is important to try to selectively transfer the magnetization from N3 to C4 while minimizing transfer to C2. After the ^{13}C-^{15}N-heteroTOCSY period, magnetization is relayed from C4 to C5 to C6 by two concatenated homonuclear refocused INEPT periods. The INEPT transfer is superior to a homonuclear ^{13}C-TOCSY transfer because of the large carbon chemical shift range (≈8500 Hz between C4 and C5) and because the INEPT allows transfer of essentially all the C4 magnetization to C6. Magnetization is then transferred to H6 for detection, where a flip-back WATERGATE sequence is used as the final refocusing period to selectively suppress the H_2O signal (Piotto et al., 1992; Grzesiek and Bax, 1993; Lippens et al., 1995; Mori et al., 1995; Mueller et al., 1995). The uridine-optimized, 2D H(NCCC)H spectrum of the leadzyme is shown in Fig. 3A, where three well-resolved HN to H6 cross peaks are observed corresponding to the three uridine residues. The uridine NH and H6 resonances have been previously assigned in the leadzyme (Legault et al., 1995), but the ability to make unambiguous through-bond connectivities for the uridine HN and H6 resonances will be an important tool for resonance assignment of other ^{13}C-/^{15}N-labeled nucleic acids. The spectrum in Fig. 3A was acquired in only 3 h, demonstrating the very high sensitivity of the 2D H(NCCC)H experiment. Further details of the acquisition and processing parameters are given in the legends to Figs. 2 and 3.

Since the H(NCCC)H transfer pathway is the same in both uridines and cytidines (see Fig. 1B), the pulse sequence in Fig. 2A can also be used to obtain through-bond H_2N to H6 connectivities in cytidines. The cytidine amino protons undergo chemical exchange by rotation about the C-N bond. This leads to less efficient transfer of heteronuclear magnetization for a ^{1}H-^{15}N-refocused INEPT sequence when compared with a heteroTOCSY sequence (data not shown) (Krishnan and Rance, 1995; Yamazaki et al., 1995). Therefore, for the identification of H_2N to H6 connectivities in cytidines the ^{1}H-^{15}N-refocused INEPT period in Fig. 2A was replaced by a ^{1}H-^{15}N-heteroTOCSY period, as depicted in Fig. 2B. Figure 3B shows a part of the cytidine-optimized 2D H(NCCC)H spectrum of the leadzyme, with the full spectrum plotted in the inset in Fig. 3C. In this spectrum the H_2N resonances are frequency labeled in ω_1 and the H6 resonances are frequency labeled in ω_2. Since the two amino proton resonances in cytidine residues are usually in slow exchange on the NMR chemical shift time scale, two cross peaks are observed for each H6 resonance. The H6 resonances and most of the C amino proton resonances have been previously assigned in the leadzyme by standard

NOE techniques (Legault, 1995) and these assignments are indicated in Fig. 3. From the 2D H(NCCC)H spectrum in Figs. 3B and 3C, we identified the H_2N to H6 connectivities for seven of the eight cytidines in the leadzyme. Connectivities were not unambiguously identified for C6, possibly because it forms an A^+-C base pair with residue 25 (Legault and Pardi, 1994), or because of exchange broadening arising from the known microsecond dynamics at the active site of the leadzyme (Legault, 1995).

One limitation of this 2D H(NCCC)H spectrum of the leadzyme is that four cytidine residues (C2, C10, C11 and

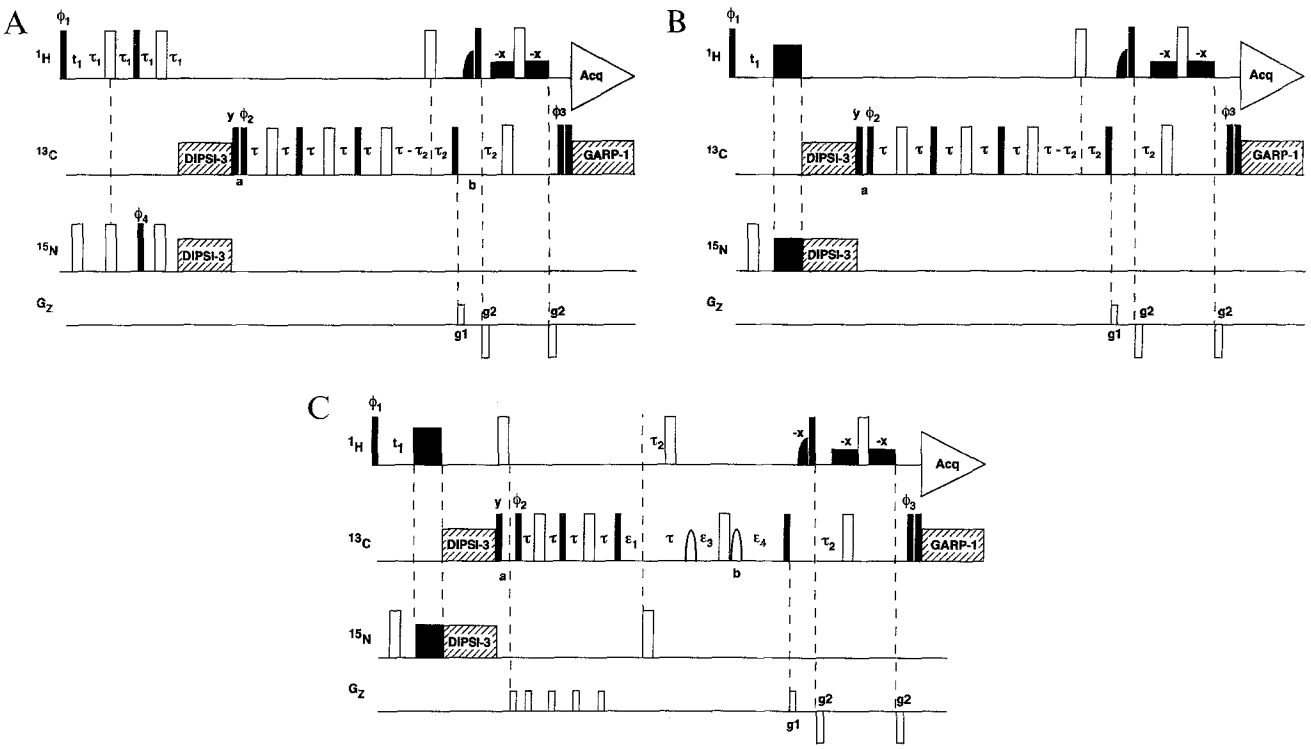

Fig. 2. Pulse sequences for the 2D and pseudo-3D HNCCCH experiments. The 90° and 180° pulses are indicated by filled and open rectangles, respectively. (A) The uridine-optimized 2D H(NCCC)H experiment, employing a refocused INEPT sequence for the ^{1}H-^{15}N transfer. The ^{1}H carrier is placed at the center of the imino proton region (13.2 ppm for uridine) at the beginning of the experiment and shifted to the water frequency at point a. A 90 ms DIPSI-3 ^{13}C-^{15}N-heteroTOCSY mixing period was used at an rf field strength of 1.9 kHz, using ^{13}C and ^{15}N carrier frequencies of 169 and 160 ppm, respectively. The ^{13}C carrier was shifted to 139 ppm at point a. Water magnetization returns to the +z-axis by radiation damping during the 90 ms ^{13}C-^{15}N-heteroTOCSY period. After this ^{13}C-^{15}N-heteroTOCSY period, the magnetization is transferred from C4 to H6 using a string of concatenated ^{13}C-^{13}C and ^{13}C-^{1}H INEPT-type transfers. The second half of the ^{13}C-^{1}H reverse INEPT transfer has been adapted to include a WATERGATE solvent peak suppression sequence (Piotto et al., 1992). In this scheme the proton 90° pulse in the center of this reverse INEPT period is preceded by a selective water flip-back 90° E-BURP pulse (2.8 ms) at point b (Geen and Freeman, 1991; Grzesiek and Bax, 1993). In the final refocused INEPT interval, the proton 180° pulse is flanked by two square 1.67 ms 90° pulses of phase –x, and the carbon 180° pulse is placed at the interval $\tau_2 = 1/(4 * {}^1J_{CH})$ following the proton 90° pulse. The phases of the selective square 90° pulses and the 90° E-BURP pulse are further optimized for maximum solvent peak suppression, using a small angle phase shifter. The transfer delays were $\tau = 3.6$ ms, $\tau_1 = 2.5$ ms and $\tau_2 = 1.25$ ms. G_z denotes the z-axis pulsed-field gradients with the following values: g1 = 300 μs at 24 G/cm and g2 = 450 μs at 32 G/cm. A 400 μs recovery time was added after each gradient. Quadrature detection in the proton t_1 period was obtained with the TPPI-States method (Marion et al., 1989). Unless otherwise noted, all pulses have phase = x. The 16-step phase cycle is: ϕ_1 = x,–x; ϕ_2 = y,y,–y,–y; ϕ_3 = 4(x),4(–x); ϕ_4 = 8(x),8(–x) and receiver = 2(x,–x,–x,x),2(–x,x,x,–x). (B) The cytidine-optimized 2D H(NCCC)H experiment, where the ^{1}H-^{15}N refocused INEPT period in the pulse sequence given in (A) is replaced with a ^{1}H-^{15}N-heteroTOCSY period. A 7.5 ms half DIPSI-3 (R,–R supercycle) sequence (Shaka et al., 1988) was used for the ^{1}H-^{15}N-heteroTOCSY transfer at an rf field strength of 1.9 kHz with the ^{15}N carrier frequency set to 96.7 ppm and the ^{1}H carrier before point a set to 7.6 ppm. Other changes compared to the pulse sequence given in (A) were that the ^{13}C-^{15}N-heteroTOCSY period was set to 45 ms ($^1J_{NC} \approx 20$ Hz for cytidine instead of ≈ 10 Hz for uridine) and an eight-step phase cycle was used, with: ϕ_1 = x,–x; ϕ_2 = y,y,–y,–y; ϕ_3 = 4(x),4(–x); and receiver = x,–x,–x,x. (C) The cytidine-optimized pseudo-3D H(NCC)CH experiment, where both the amino proton resonances and the C6 resonances are frequency labeled during the t_1 evolution periods. The parameters for the cytidine-optimized pseudo-3D H(NCC)CH were the same as those for the cytidine-optimized 2D H(NCCC)H, except that the ^{13}C carrier was positioned at 129 ppm at point a and two 1.03 ms frequency-shifted selective IBURP 180° ^{13}C pulses (Geen and Freeman, 1991; Patt, 1992) were applied at 104 ppm. The first selective pulse is used to decouple C5 from C6 during the time-shared ^{13}C evolution period and the second pulse at point b compensates for off-resonance effects caused by the first selective 180° pulse (Grzesiek and Bax, 1992). The C6 evolution period t_1 is time shared with both the $2 * \tau$ period that refocuses the C5-C6 antiphase component and the $2 * \tau_2$ period that creates the C6-H6 antiphase component (Logan et al., 1993). The time periods ε_1, ε_3 and ε_4 were set to 0, 0 and τ, respectively, for the initial t_1 interval. For evolution of the C6 chemical shift during the t_1 period, the increments of these intervals are: $\delta\varepsilon_1 = dw/2$, $\delta\varepsilon_3 = (dw/2 - \tau/(n+1))$, and $\delta\varepsilon_4 = -\tau/(n+1)$, were dw is the dwell time and n is the total number of points in the t_1 dimension. The ^{1}H 180° pulse at point a is used to invert the water magnetization and the five gradient pulses subsequently eliminate radiation damping and keep the water magnetization aligned along the –z-axis until the next ^{1}H 180° pulse flips the water signal back to the +z-axis.

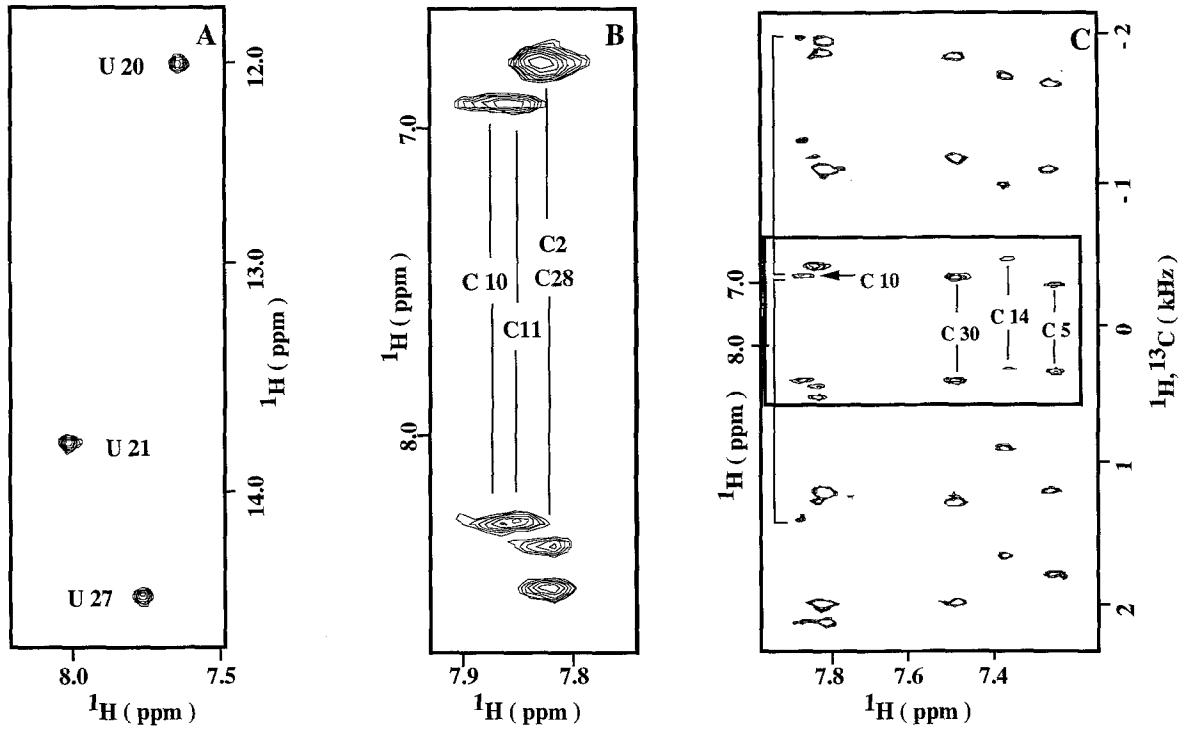

Fig. 3. Contour plots of (A) the uridine-optimized 2D H(NCCC)H spectrum; (B) part of the cytidine-optimized 2D H(NCCC)H spectrum; and (C) the cytidine-optimized pseudo-3D H(NCC)CH spectrum of the leadzyme. The full cytidine-optimized 2D H(NCCC)H spectrum is given in the inset in (C). These spectra were acquired with the pulse sequences given in Fig. 2. Both 2D spectra were collected with spectral widths in ω_1 and ω_2 of 2000 and 6000 Hz, respectively, 80 complex t_1 points, 512 complex t_2 points, 64 scans per FID and a relaxation delay of 1.1 s for a total acquisition time of 3 h. The pseudo-3D spectrum was collected with the spectral widths in ω_1 and ω_2 both set to 6000 Hz, 200 complex t_1 points, 512 complex t_2 points, 64 scans per FID and a relaxation delay of 1.1 s for a total acquisition time of 8 h. ^{13}C decoupling during t_2 was achieved with GARP-1 at an rf field strength of 1.6 kHz. All experiments were performed on a 1.8 mM 99% ^{13}C-/^{15}N-labeled RNA sample at 15 °C on a Varian Unityplus 500 MHz spectrometer. Data were transferred to a Silicon Graphics Indigo^2 computer and processed with the program FELIX, v. 2.35 (Biosym Technologies Inc., San Diego, CA).

C28) have very similar H6 and amino proton chemical shifts (see Fig. 3B). To overcome this problem, the 2D H(NCCC)H pulse sequence in Fig. 2B can be extended into additional dimensions by frequency labeling of the imino/amino nitrogen, C4, C5 or C6 resonances. Since there are relatively few cross peaks in the 2D H(NCCC)H spectrum, we chose here to employ the 'reduced dimensionality' (Szyperski et al., 1993a,b; Simorre et al., 1994) approach and to acquire a pseudo-3D experiment. The pulse sequence for the pseudo-3D H(NCC)CH experiment is shown in Fig. 2C. This sequence is a modification from the one in Fig. 2B by adding a second t_1 evolution time while the magnetization is on the C6 carbon and by incrementing this period simultaneously with the first t_1 period. Although these HNCCCH experiments have a very high sensitivity, to help reduce the effects of transverse relaxation during the carbon evolution period, we have also incorporated the time-shared evolution procedure of Fesik and co-workers (Logan et al., 1993). The time-shared evolution procedure employed here is more complicated than previous versions (Logan et al., 1993), because three time periods, the carbon t_1 evolution, the $1/(2J_{CH})$ period and the $1/(2J_{CC})$ period, are being concatenated. In this time-shared evolution procedure the C6 chemical shift evolves during the time $(\varepsilon_1+\tau+PW_I+\varepsilon_3-PW_I-\varepsilon_4)$, which corresponds to the t_1 period, and where PW_I is the length of the IBURP2 180° carbon pulse. The $^1J_{CC}$ coupling constant evolves during the time $(\varepsilon_1+\tau-\varepsilon_3+\varepsilon_4)$, which corresponds to $1/(2J_{CC})$ for every t_1 period. The $^1J_{CH}$ coupling constant evolves during the time $(\varepsilon_1+2*\tau_2-\tau-PW_I-\varepsilon_3+PW_I+\varepsilon_4)$, which corresponds to $1/(2J_{CH})$ for every t_1 period. The $^1J_{CN}$ coupling constant is decoupled during the time-shared evolution period. The ε_1, ε_3 and ε_4 times are initially set to 0, 0 and τ, respectively, where $\tau=1/(4J_{CC})$. For each t_1 point these times are incremented by dw/2, $[dw/2-\tau/(n+1)]$ and $-\tau/(n+1)$, respectively, where dw corresponds to the dwell time and n to the total number of points in the t_1 dimension. One frequency-shifted selective IBURP2 (Geen and Freeman, 1991; Patt, 1992) carbon 180° pulse is applied to the C5 resonances in the middle of the carbon evolution to eliminate the homonuclear C5-C6 coupling during the carbon t_1 period. A second IBURP2 carbon 180° pulse is applied at point b, which allows the C5-C6 coupling to evolve for a time period $1/(2J_{CC})$ and also compensates for off-resonance effects caused by the first selective 180° pulse (Grzesiek and Bax, 1992). For the longest t_1 value, this procedure reduces the time that the carbon magnetization

spends in the transverse plane by $1/(2J_{CC}) = 7.2$ ms, and therefore should improve the sensitivity of the experiment in larger RNAs. Further details of the implementation of the time-shared evolution procedure are given in the legend to Fig. 2.

Figure 3C shows the aromatic region of the cytidine-optimized pseudo-3D H(NCC)CH spectrum of the leadzyme. In this experiment quadrature detection was performed in the proton t_1 evolution period, so that peaks are observed at $\omega_H \pm \omega_C$. For reference, the cytidine-optimized 2D H(NCCC)H spectrum of the leadzyme is shown in the inset in the figure. In the pseudo-3D H(NCC)CH spectrum, an H6 resonance shows four cross peaks in ω_1 because each amino proton is split into a pair of cross peaks. For each pair of cross peaks the position midway between the pair corresponds to the frequency of that amino proton, and the frequency difference between these cross peaks corresponds to twice the frequency difference of the C6 carbon resonance from the carbon carrier (Szyperski et al., 1993a,b; Simorre et al., 1994). Thus, ω_1 contains chemical shift information for both the amino protons and the C6 carbons. Analysis of both the 2D and pseudo-3D spectra of the leadzyme shows that some cross peaks that are not resolved in one experiment are resolved in the other. This pseudo-3D approach is not limited to frequency labeling of the C6 carbons; instead, either the amino/imino nitrogens, C4 carbons or C5 carbons could be frequency labeled along with the amino/imino protons in t_1.

The spectra in Fig. 3 have a very high sensitivity, with the 2D spectra acquired in only 3 h and the pseudo-3D spectrum in 8 h at 500 MHz on a 1.8 mM RNA sample. Thus, these experiments are very efficient; however, there are many other pulse sequences that can be designed to identify these HN/H_2N to H6 connectivities. We tested a variety of H(NCCC)H pulse sequences in ^{13}C-/^{15}N-labeled mono- and oligonucleotides and found that for the molecules studied, the most efficient pulse sequences are those in Fig. 1. For example, the N4 to C4 magnetization transfer in cytidine can be accomplished by an INEPT-type sequence instead of the ^{13}C-^{15}N-heteroTOCSY sequence employed here, and this experiment has similar sensitivity to those given here (data not shown). The N3 to C4 magnetization transfer in uridine can also be accomplished by an INEPT sequence (data not shown), but this requires the use of very selective carbon pulses to eliminate transfer from N3 to C2. Where relaxation becomes a significant problem, the uridine-optimized 2D H(NCCC)H pulse sequence in Fig. 2A can be modified to include the time-shared evolution procedure during the proton t_1 period (Logan et al., 1993). This concatenation of the t_1 and $(1/J_{HN})$ periods (Logan et al., 1993) should lead to higher sensitivity of the uridine-optimized 2D H(NCCC)H experiment for larger RNAs.

The 2D and pseudo-3D HNCCCH experiments presented here provide unambiguous identification of the uridine HN to H6 and cytidine H_2N to H6 connectivities in ^{13}C-/^{15}N-labeled nucleic acids. This set of HNCCCH experiments provides a very efficient means for making unambiguous through-bond connectivities for pyrimidine bases. Sequential assignments of the exchangeable imino and amino protons in nucleic acids are generally made independent of the assignment of the nonexchangeable base and sugar protons (Wijmenga et al., 1993; Pardi, 1995). Thus, the through-bond HN/H_2N to H6 connectivities identified here represent an important bridge between assignment of exchangeable and nonexchangeable protons by directly linking the sequential assignment pathways for the exchangeable (HN and H_2N) protons and the nonexchangeable (H6) protons in nucleic acids. These experiments, in combination with other recently developed through-bond experiments (Pardi, 1995), greatly facilitate the resonance assignment of isotopically labeled nucleic acids.

Acknowledgements

This work was supported by NIH Grant AI33098 and a Research Career Development Award AI01051 to A.P., and a NATO/CNRS Fellowship to J.P.S. We thank the Colorado RNA Center and the W.M. Keck Foundation for their generous support of RNA research on the Boulder campus, and Dr. Pascale Legault for providing the leadzyme sample and for helpful discussions.

References

Batey, R.T., Inada, M., Kujawinski, E., Puglisi, J.D. and Williamson, J.R. (1992) *Nucleic Acids Res.*, **20**, 4515–4523.

Bertrand, R.D., Moniz, W.B., Garroway, A.N. and Chingas, G.C. (1978) *J. Am. Chem. Soc.*, **100**, 5227–5229.

Dieckmann, T. and Feigon, J. (1994) *Curr. Opin. Struct. Biol.*, **4**, 745–749.

Farmer II, B.T., Mueller, L., Nikonowicz, E.P. and Pardi, A. (1993) *J. Am. Chem. Soc.*, **115**, 11040–11041.

Farmer II, B.T., Mueller, L., Nikonowicz, E.P. and Pardi, A. (1994) *J. Biomol. NMR*, **4**, 129–133.

Geen, H. and Freeman, R. (1991) *J. Magn. Reson.*, **93**, 93–141.

Grzesiek, S. and Bax, A. (1992) *J. Am. Chem. Soc.*, **114**, 6291–6293.

Grzesiek, S. and Bax, A. (1993) *J. Am. Chem. Soc.*, **115**, 12593–12594.

Heus, H.A., Wijmenga, S.S., Van de Ven, F.J.M. and Hilbers, C.W. (1994) *J. Am. Chem. Soc.*, **116**, 4983–4984.

Kellogg, G.W., Szewczak, A.A. and Moore, P.B. (1992) *J. Am. Chem. Soc.*, **114**, 2727–2728.

Krishnan, V.V. and Rance, M. (1995) *J. Magn. Reson. Ser. A*, **116**, 97–106.

Legault, P., Farmer II, B.T., Mueller, L. and Pardi, A. (1994) *J. Am. Chem. Soc.*, **116**, 2203–2204.

Legault, P. and Pardi, A. (1994) *J. Am. Chem. Soc.*, **116**, 8390–8391.

Legault, P. (1995) Ph.D. Thesis, University of Colorado, Boulder, CO.

Legault, P., Jucker, F.M. and Pardi, A. (1995) *FEBS Lett.*, **362**, 156–160.

Lippens, G., Dhalluin, C. and Wieruszeski, J.M. (1995) *J. Biomol. NMR*, **5**, 327–331.

Logan, T.M., Olejniczak, E.T., Xu, R.X. and Fesik, S.W. (1993) *J. Biomol. NMR*, **3**, 225–231.

Marino, J.P., Prestegard, J.H. and Crothers, D.M. (1994a) *J. Am. Chem. Soc.*, **116**, 2205–2206.

Marino, J.P., Schwalbe, H., Anklin, C., Bermel, W., Crothers, D.M. and Griesinger, C. (1994b) *J. Am. Chem. Soc.*, **116**, 6472–6473.

Marino, J.P., Schwalbe, H., Anklin, C., Bermel, W., Crothers, D.M. and Griesinger, C. (1995) *J. Biomol. NMR*, **5**, 87–92.

Marion, D., Ikura, M., Tschudin, R. and Bax, A. (1989) *J. Magn. Reson.*, **85**, 393–399.

Mori, S., Abeygunawardana, C., Johnson, M.O. and Van Zijl, P.C.M. (1995) *J. Magn. Reson. Ser. B*, **108**, 94–98.

Morris, G.A. and Freeman, R. (1979) *J. Am. Chem. Soc.*, **101**, 760–762.

Mueller, L. and Ernst, R.R. (1979) *Mol. Phys.*, **38**, 963–992.

Mueller, L., Legault, P. and Pardi, A. (1995) *J. Am. Chem. Soc.*, **117**, 11043–11048.

Nikonowicz, E.P., Sirr, A., Legault, P., Jucker, F.M., Baer, L.M. and Pardi, A. (1992) *Nucleic Acids Res.*, **20**, 4507–4513.

Nikonowicz, E.P. and Pardi, A. (1993) *J. Mol. Biol.*, **232**, 1141–1156.

Pan, T. and Uhlenbeck, O.C. (1992) *Nature*, **358**, 560–563.

Pardi, A. and Nikonowicz, E.P. (1992) *J. Am. Chem. Soc.*, **114**, 9301–9302.

Pardi, A. (1995) *Methods Enzymol.*, **261**, 350–380.

Patt, S.L. (1992) *J. Magn. Reson.*, **96**, 94–102.

Piotto, M., Saudek, V. and Sklenář, V. (1992) *J. Biomol. NMR*, **2**, 661–665.

Shaka, A.J., Lee, C.J. and Pines, A. (1988) *J. Magn. Reson.*, **77**, 274–293.

Simorre, J.P., Brutscher, B., Caffrey, M.S. and Marion, D. (1994) *J. Biomol. NMR*, **4**, 325–333.

Sklenář, V., Peterson, R.D., Rejante, M.R. and Feigon, J. (1993a) *J. Biomol. NMR*, **3**, 721–727.

Sklenář, V., Peterson, R.D., Rejante, M.R., Wang, E. and Feigon, J. (1993b) *J. Am. Chem. Soc.*, **115**, 12181–12182.

Szyperski, T., Wider, G., Bushweller, J.H. and Wüthrich, K. (1993a) *J. Biomol. NMR*, **3**, 127–132.

Szyperski, T., Wider, G., Bushweller, J.H. and Wüthrich, K. (1993b) *J. Am. Chem. Soc.*, **115**, 9307–9308.

Tate, S., Ono, A. and Kainosho, M. (1994) *J. Am. Chem. Soc.*, **116**, 5977–5978.

Wijmenga, S.S., Mooren, M.M.W. and Hilbers, C.W. (1993) In *NMR of Macromolecules* (Ed., Roberts, G.C.K.), Oxford University Press, Oxford, pp. 217–288.

Wijmenga, S.S., Heus, H.A., Leeuw, H.A.E., Hoppe, H., Van der Graaf, M. and Hilbers, C.W. (1995) *J. Biomol. NMR*, **5**, 82–86.

Yamazaki, T., Pascal, S.M., Singer, A.U., Forman-Kay, J.D. and Kay, L.E. (1995) *J. Am. Chem. Soc.*, **117**, 3556–3564.

Zimmer, D.P. and Crothers, D.M. (1995) *Proc. Natl. Acad. Sci. USA*, **92**, 3091–3095.